Limited Macrophage Positional Dynamics in Progressing or Regressing Murine Atherosclerotic Plaques—Brief Report

Jesse W. Williams, Catherine Martel, Stephane Potteaux, Ekaterina Esaulova, Molly A. Ingersoll, Andrew Elvington, Brian T. Saunders, Li-Hao Huang, Andreas J. Habenicht, Bernd H. Zinselmeyer, Gwendalyn J. Randolph

Objective—Macrophages play important roles in the pathogenesis of atherosclerosis, but their dynamics within plaques remain obscure. We aimed to quantify macrophage positional dynamics within progressing and regressing atherosclerotic plaques.

Approach and Results—In a stable intravital preparation, large asymmetrical foamy macrophages in the intima of carotid artery plaques were sessile, but smaller rounded cells nearer plaque margins, possibly newly recruited monocytes, mobilized laterally along plaque borders. Thus, to test macrophage dynamics in plaques over a longer period of time in progressing and regressing disease, we quantified displacement of nondegradable phagocytic particles within macrophages for up to 6 weeks. In progressing plaques, macrophage-associated particles appeared to mobilize to deeper layers in plaque, whereas in regressing plaques, the label was persistently located near the lumen. By measuring the distance of the particles from the floor of the plaque, we discovered that particles remained at the same distance from the floor regardless of plaque progression or regression. The apparent deeper penetration of labeled cells in progressing conditions could be attributed to monocyte recruitment that generated new superficial layers of macrophages over the labeled phagocytes.

Conclusions—Although there may be individual exceptions, as a population, newly differentiated macrophages fail to penetrate significantly deeper than the limited depth they reside on initial entry, regardless of plaque progression, or regression. These limited dynamics may prevent macrophages from escaping areas with unfavorable conditions (such as hypoxia) and pose a challenge for newly recruited macrophages to clear debris through efferocytosis deep within plaque.

Visual Overview—An online visual overview is available for this article. **(*Arterioscler Thromb Vasc Biol*. 2018;38:1702-1710. DOI: 10.1161/ATVBAHA.118.311319.)**

Key Words: arteriosclerosis ■ cell adhesion ■ inflammation ■ intravital microscopy ■ monocytes

Atherosclerotic disease remains one of the leading causes of morbidity and mortality in the Western world. Hallmarks of this disease include accumulation of lipids in the vessel wall and a chronic inflammatory state that is orchestrated by several immune cells, such as macrophages, dendritic cells, and T lymphocytes. In particular, recruited monocyte-derived macrophages and proliferating macrophages within the arterial wall take up cholesterol-rich lipoproteins and play a critical role in the pathogenesis of atherosclerosis by developing into foam cells.[1,2] For example, activated macrophages within early atherosclerotic plaques secrete proinflammatory cytokines and chemokines,[3] which results in the recruitment of immune cells, such as monocytes and migration of smooth muscle cells from the media into the intima. Plaque progression can eventually result in its rupture and catastrophic vessel occlusion.

See accompanying editorial on page 1671

Morphologically, atherosclerotic plaques bear some resemblance to granulomas, developing marked clusters of macrophages that can progress to incorporate a necrotic core. In atherosclerosis, necrotic core debris is a major driver of thrombotic risk and rupture.[4] An unanswered question, however, is whether the limited macrophage dynamics previously described for mycobacterial granulomas[5] applies to atherosclerotic plaques. If so, then one can envision that necrotic core formation and expansion could partly be a consequence of macrophages having limited ability to emigrate away from any microenvironment that might preferentially predispose to their death or to mobilize toward dying cells to clear them. Indeed, to use mathematical modeling in the future to predict plaque dynamics that lead to stable or unstable lesions requires that, we understand how well macrophages are able to move around within plaques in different conditions.

Received on: January 6, 2018; final version accepted on: May 22, 2018.

From the Department of Pathology & Immunology, Washington University School of Medicine, St Louis, MO (J.W.W., C.M., E.E., A.E., B.T.S., L.-H.H., B.H.Z., G.J.R.); Department of Gene and Cell Medicine, Mount Sinai School of Medicine, New York (S.P., M.A.I., G.J.R.); and Institute for Cardiovascular Prevention, Ludwig Maximilians University of Munich, Germany (A.J.H.).

Current address for C. Martel: Department of Medicine, Montreal Heart Institute, Quebec, Canada.

Current address for S. Potteaux: INSERM Unit 970, Paris, France.

Current address for M.A. Ingersoll: Department of Immunology, Pasteur Institute and INSERM U1223, Paris, France.

Current address for A. Elvington: Division of Health and Sport Sciences, Missouri Baptist University, St Louis, MO.

The online-only Data Supplement is available with this article at https://www.ahajournals.org/journal/atvb/doi/suppl/10.1161/atvbaha.118.311319.

Correspondence to Gwendalyn J. Randolph, PhD, Department of Pathology & Immunology, 425 S Euclid Ave, Box 8118, Washington University School of Medicine, St Louis, MO 63110. E-mail gjrandolph@wustl.edu

Nonstandard Abbreviations and Acronyms	
ApoE	apolipoprotein E
GFP	green fluorescent protein
HFD	high-fat diet

To address the issue of defining macrophage dynamics in plaque, we undertook a 2-pronged approach modeled after that used by Egen et al,[5] first using intravital imaging to examine macrophage behavior in the living mouse and then adding a second approach to track cells over a much longer period of time than is possible with intravital imaging. Intravital 2-photon microscopy has advanced our understanding of immune responses during steady state and in a wide variety of disease models, and some recent advances have been made in imaging atherosclerotic disease using this technique.[6–11] Here, we have applied a stable and high-resolution imaging approach to visualize native atherosclerotic plaques in the carotid artery to allow for short-term observation of macrophage motility within the developing plaque. In addition, for long-term assessment of macrophage positioning, we quantified the location of stable phagocytic cargo carried by macrophages within plaques during progressive or regressive atherosclerotic disease. Use of phagocytic cargo with differing fluorescent colors at different time points supported the conclusion that macrophages within the atherosclerotic plaques are largely sessile cells, regardless of plaque progression or regression. Macrophages seem especially unlikely to deeply penetrate plaques, such that successive waves of recruited monocytes create layers somewhat reminiscent of growth rings in trees.

Methods

The data that support the findings of this study are available from the corresponding author upon reasonable request.

Mice

LysM$^{cre/+}$ (B6.129P2-Lyz2$^{tm1(cre)Ifo}$/J, Jackson Laboratories, No. 004781), Rosa$^{Lsl\text{-}Tomato}$ (B6; 129S6-Gt(ROSA)26Sor$^{tm9(CAG\text{-}tdTomato)Hze}$/J, Jackson Laboratories, No. 007905), Ldlr$^{-/-}$ (B6.129S7-Ldlr^{tm1Her}/J, Jackson Laboratories, No. 002207), and B6 Apoe$^{-/-}$ (B6.129P2-Apoe^{tm1Unc}/J, Jackson Laboratories, No. 002052) mice were purchased from The Jackson Laboratories and then bred at Washington University or Mount Sinai. CCR2$^{gfp/+}$ (B6(C)-Ccr2$^{tm1.1Cln}$/J, Jackson Laboratories No. 027619)[12] mice were kindly provided by Dr Marco Colonna (Washington University in St Louis). Strains were crossed for intravital imaging to generate LysM$^{cre/+}$ Rosa$^{LSL\text{-}Tomato}$ Ldlr$^{-/-}$ and CCR2$^{gfp/+}$ Ldlr$^{-/-}$ mice, whereas Apoe$^{-/-}$ mice were used for progression and regression studies. For atherosclerosis studies, mice were placed on a high-fat diet (HFD; 21% milk fat, 0.15% cholesterol; Envigo Teklad TD.88137) at the age of 6 weeks for 12 to 16 weeks. For all progression studies (including intravital imaging), both male and female mice were used and combined for analysis. For microarray analysis, male mice were used. Regression experiments using the adeno-associated viral 8 ApoE (apolipoprotein E) vector (Vector Biolabs) showed a low infection efficacy in female animals; therefore, male mice were used for studies involving reversal of hypercholesterolemia. However, regression studies involving use of adenovirus encoding hApoE3 (gift from Dr Dan Rader) were performed in female mice. All animal procedures were approved by the Institutional Animal Care and Use Committee at Washington University School of Medicine, St Louis, Missouri or Mount Sinai School of Medicine, New York, NY.

Two-Photon Microscopy and Data Analysis

For intravital carotid imaging, after 12 to 16 weeks HFD feeding, hair was removed using a depilatory cream and a small neck incision was opened to expose the carotid artery. Plaque regions in close proximity to the common carotid bifurcation were gently elevated out of the cavity and placed under an adjustable coverslip for stability and to facilitate access of the microscope's objective. Imaging was performed on a modified Leica SP8 2-photon imaging system with a custom temperature controlled hood. GFP (green fluorescent protein) and tomato-labeled cells were visualized using a Mai Tai Deepsee laser (Specta Physics, Santa Clara, CA) optimally tuned to 920 and 950 nm consecutively. Fluorescence emission passed through 458, 495, and 560 nm long-pass mirrors, with the 458 and 560 placed below and above the 495. Emission was detected by ultrasensitive hybrid detectors with tomato >560 nm, GFP 495 to 560 nm, autofluorescence 458 to 495, and second harmonic <458 nm. Time-lapse recordings were acquired using Leica Application Suite, LAS X (Leica Microsystems). Twenty-five to 30 frames (2.5-µm stack size, 62.5–75 µm total) were acquired every 15 seconds. Multidimensional rendering and manual cell tracking were analyzed with Imaris (Bitplane, Zurich, Switzerland) to generate speed of migration and displacement data. Data were transferred and plotted in GraphPad Prism 6.0 (GraphPad Software Inc, La Jolla, CA)

Cellular Bead Labeling

Classical Ly-6C^{hi} monocytes were labeled with beads 3 days after intravenous injection of 250 µL clodronate-loaded liposomes (purchased at clodronateliposomes.org). One micrometer Fluoresbrite yellow-green or red fluorescent plain microspheres (Polysciences Inc, Warrington, PA) diluted 1:4 in sterile PBS were administered intravenously (200 µL). Nonclassical Ly-6C^{lo} monocytes were labeled with beads similarly, but without the use of clodronate-loaded liposomes.[13] Labeling efficiency of blood monocytes was verified by flow cytometry 1 day after labeling.

Atherosclerosis Development and Plaque Regression After Viral Vector-Induced Expression of ApoE

At the age of 5 to 6 weeks, ApoE$^{-/-}$ mice were transitioned to a high fat, cholesterol-enriched diet (Envigo Teklad TD.88137) and maintained on this diet for an additional 12 to 16 weeks, as indicated. In some experiments, matched cohorts of mice were divided into 3 groups. In all groups, monocytes were labeled with fluorescent beads as described above. Then, 5 to 8 days later, 1 group was euthanized as a baseline cohort. The 2 other groups remained on a HFD for an additional 4 to 6 weeks and were infected either with ApoE-encoding adenoviral vector (ad-hApoE3) to rapidly reduce total plasma cholesterol and induce regression of plaque macrophages[13–15] or with its control empty adenoviral vector intravenously. Experiments were repeated using adeno-associated viral-hApoE3 (Vector Biolabs). Infection with the ApoE vector was routinely verified in each animal by measuring reduction of total cholesterol levels after blood collection at the submandibular vein. After euthanasizing, mice were perfused with 4% paraformaldehyde-saline, hearts were isolated, and tissue was fixed in a solution of 4% paraformaldehyde and 30% sucrose. Tissue was embedded in optimal cutting temperature compound (Tissue-Tek), and 10 µm cryosections were made spanning the depth of the entire aortic sinus. Images of plaque sections prepared at the aortic sinus were collected using a Nikon E800 bright field microscope, and the fluorescent bead number in plaque was counted using a Leica SPE confocal microscope. Image J software was used to assess the distance that each bead in plaque sections was positioned relative to the luminal endothelial surface and, separately, to the floor of the plaque demarcated by elastic lamina and a smooth muscle cell layer.

Gene Expression Analysis

As described above, C57Bl/6 mice were injected intravenously with latex beads (diluted 1:4 in PBS) 3 days after clodronate-loaded

liposome mediate monocyte depletion. Then 4 days later, classical and nonclassical blood monocytes were fluorescence-activated cell sorter sorted (FACSAria, BD Biosciences) for presence or absence of latex beads. RNA was extracted from sorted cells using TRIzol and RNeasy mRNA isolation kit (Qiagen). RNA amplification, direct labeling, hybridization, and chip scanning were performed as previously described.[16] Microarray was performed on an Affymetrix GeneChip 430 2.0. R packages Oligo and Limma were used to read the microarray expression data, normalize, access QC, and perform DE. Gene set enrichment analysis with fgsea package was used to probe for pathway enrichment in hallmark and canonical pathways. Benjamini-Hochberg correction was used to correct *P* value for multiple comparisons. Gene expression data were submitted to the Gene Expression Omnibus data bank (accession number GSE117051).

Statistics

Values are presented as the mean±SEM. Data were assessed for homogeneity of variance by Bartlett test. Samples not conforming to equal variance were assayed by Kruskal-Wallis rank test, where adjusted *P* values <0.05 was considered significant (*P* value, *≤0.05, **≤0.01, ***≤0.001, and ****≤0.001). For samples conforming to equal variance, data were analyzed further by 2-tailed ANOVA with Tukey correction for multiple comparison, where a *P* value <0.0332 was considered significant (*P* value, *≤0.0332, **≤0.0021, ***≤0.0002, and ****≤0.00 001).

Results

Visualization of Monocytes and Monocyte-Derived Macrophages in Atherosclerotic Plaques

Stable intravital imaging of the carotid artery of plaque-bearing LysM$^{cre/+}$ Rosa$^{LSL\text{-}Tomato}$ Ldlr$^{-/-}$ mice was performed to examine intraplaque macrophage motility. As illustrated by 3-dimensional image reconstruction, the preparation allowed for examination through the vessel wall to visualize plaque and the lumen of the artery (Figure 1A). Acellular necrotic regions within plaques, commonly associated with late-stage atherosclerosis, were not observed in the carotid artery after 12- to 16-week HFD feeding. Tomato-expressing asymmetrical cells, resembling foamy macrophages based on size, location and morphology, were the primary cell type present in the carotid plaques (Figure 1A; Movie I in the online-only Data Supplement). Asymmetrical morphology is a consistent feature of cells that have undergone transendothelial migration and, therefore, are within the plaque intima region.[17] Similarly, cells with a more rounded symmetrical morphology are potentially within the vasculature and interacting with the endothelial surface.

Plaque macrophages, identified as indicated by asymmetrical morphology and expression of the fluorescent

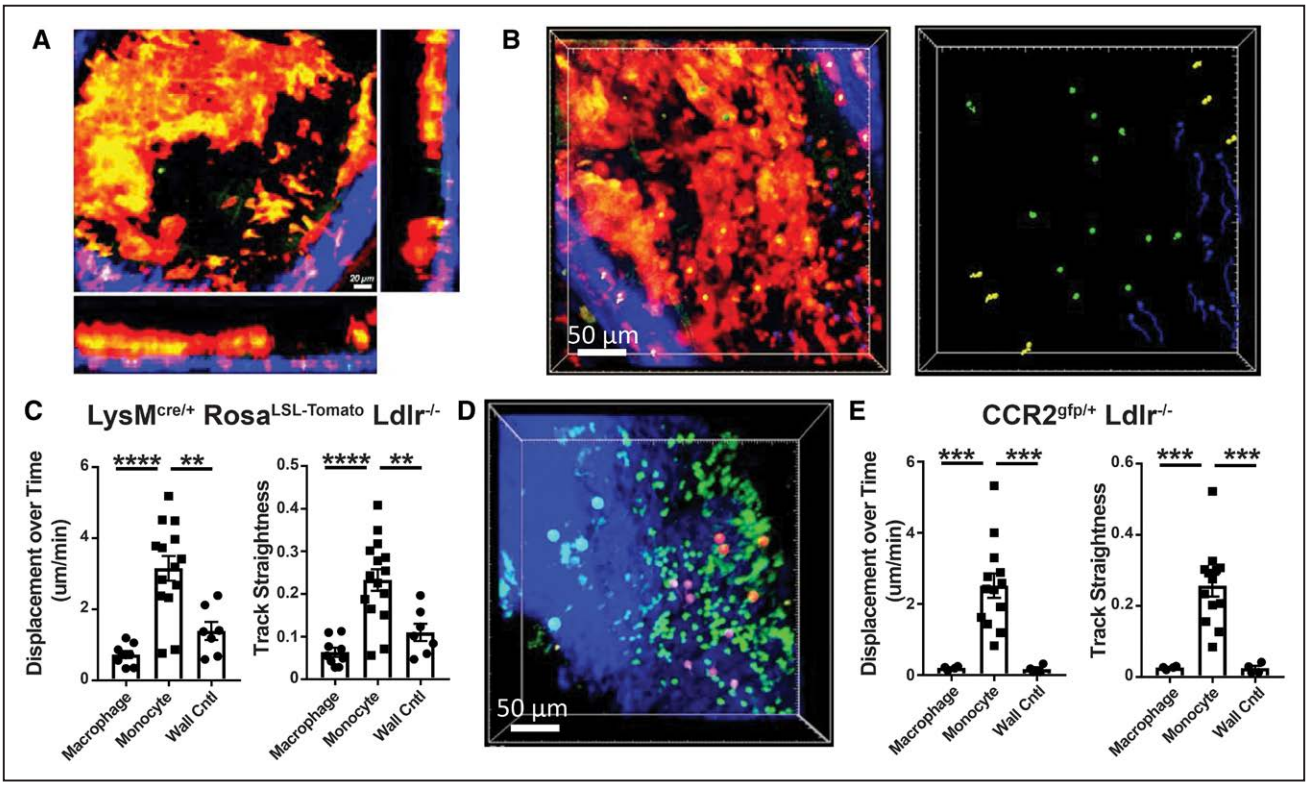

Figure 1. Three dimensional-myeloid cell dynamics within established atherosclerotic plaque using intravital imaging. **A**, Image from intravital imaging from the carotid artery of plaque-bearing LysM$^{cre/+}$ Rosa$^{LSL\text{-}Tomato}$ Ldlr$^{-/-}$ mouse showing established plaque myeloid cells (red), arterial wall (blue, second harmonic signaling), and lumen (black). Green is autofluorescent background signal. **B**, Foamy macrophages within the plaque (identified by large Tomato^{+} asymmetrical cells found within the lumen of the plaque, identified with green balls), monocytes (small Tomato^{+} symmetrical cells found on plaque boarders, identified with blue balls), and macrophages within the arterial wall (Tomato^{+} cells found in the wall of the artery, identified with yellow balls) were charted for their motility >10 min of continuous imaging. Cell tracks were assayed for (**C**) displacement length over time and track straightness (track displacement/track length). **D**, CCR2$^{gfp/+}$ Ldlr$^{-/-}$ mice were used to track intraplaque dynamics after 12 wk high-fat diet feeding. Foamy macrophages (identified by orange balls), monocytes (purple balls), and wall macrophages (blue balls) were used to track cell dynamics >1 h of continuous imaging, and plotted for (**E**) displacement/time and track straightness. Data are representative from individual videos that are representative of at least 4 independent experiments for each model. Statistical significance was assayed by Kruskal-Wallis rank test where adjusted *P* values <0.05 was considered significant (*P* value, *≤0.05, **≤0.01, ***≤0.001, and ****≤0.001).

Td-Tomato molecule, were observed to be particularly sessile during intravital imaging. However, a particular pattern of motility was evident during intravital 2-photon microscopy of progressive plaques (Movie I in the online-only Data Supplement). This motility appeared to be restricted to the smaller-sized and symmetrical Tomato$^+$ cells, resembling monocytes, and motility appeared to be distinct to regions on plaque borders. Migration on the plaque border is consistent with the proposed primary location of monocyte recruitment to plaque.[18–20] Tomato-labeled asymmetrical (marked by green dots) and symmetrical, rounded cells (marked by blue dots) were charted for trajectories of individual cells over a 10-minute video segment (Figure 1B and 1C). To control for movement associated with the live animal preparation, motility was compared against Tomato$^+$ asymmetrical cells observed in the outer arterial wall and not in the plaque as a control for vibrations associated with heartbeat and blood flow, labeled by yellow dots. Dots used to label cells in videos are overlaid with a 3D image, therefore, bead color (particularly the green beads) merge to appear yellow in the overlay, left panel of Figure 1B. Correct bead colors can be seen on the right panel of Figure 1B; Movie I in the online-only Data Supplement). Asymmetrical cells found within plaque displayed little net displacement over the imaging period, and no significant migratory potential over control cells identified in the wall (Figure 1C and 1D). This is consistent with fully differentiated macrophages within many other tissues where they are thought to be nonmotile cells. Furthermore, the motion detected in asymmetrical cells was not directed movement and showed little straightness (net displacement/track length; Figure 1C). By contrast, the small symmetrical Tomato$^+$ cells outside of the main plaque area, but near the plaque border, showed marked displacement and a high degree of directed motility over the imaging period. Thus, the Tomato$^+$ cells in plaques could be divided into 2 populations based on behavior, with central macrophages, resembling foamy macrophages, in the high cellular density areas of plaque exhibiting minimal motility and a second population, resembling monocytes, on the plaque periphery showing high motility. A few small Tomato+ cells were also nonmotile, suggestive of the possibility that these cells were recently recruited across the endothelial layer and were still undergoing differentiation into mature macrophages in tissue. Unfortunately, the limited continuous imaging time did not allow for observation of these cells transitioning to mature foam cells. Regardless of this caveat, these observations support a concept that differentiation of monocytes to macrophages in plaque yields macrophages with limited displacement potential.

The LysM^{cre} reporter system is an efficient approach for labeling macrophages within atherosclerotic plaque. However, it introduces difficulty in separating neutrophils from monocytes. By flow cytometric analysis, both neutrophil and monocytes express the fluorescent Tomato protein in LysM$^{cre/+}$ Rosa$^{LSL\text{-}Tomato}$ Ldlr$^{-/-}$ mice (Figure IA and IB in the online-only Data Supplement). This raises the possibility that small migratory cells observed in and around foamy macrophages in Figure 1A through 1C could potentially be neutrophils and not monocytes as anticipated. To confirm whether monocytes were the motile cells observed in our intravital preparations, we used the CCR2$^{gfp/+}$ Ldlr$^{-/-}$ reporter mouse,[12] where blood monocytes, but no other blood cell, expressed GFP (Figure IB in the online-only Data Supplement). This mouse was suitable for intravital imaging and the GFP label also identified a small subset, but not all macrophages within the atherosclerotic plaque (Figure 1D; Figure IC in the online-only Data Supplement). Performing intravital imaging on CCR2$^{gfp/+}$ Ldlr$^{-/-}$ mice fed HFD for 12 weeks showed similar kinetics as seen in our previous model (Movie II in the online-only Data Supplement). Asymmetrical macrophages displayed sessile behavior, but small rounded symmetrical cells (in this scenario, monocytes) were observed to be motile on the plaque borders. Importantly, the monocytes displayed the same relative displacement/time and straightness measurements as found in our previous LysM$^{cre/+}$ Tomato-expressing model (Figure 1E). These features of plaque were observed in both male and female mice. Together, these data suggest that motile monocytes migrate into and along plaque borders, but that macrophages that have undergone transendothelial migration into plaque regions display limited motility, at least during acute time periods of intravital imaging.

Recruited Monocytes Deposit on the Surface and Do Not Penetrate Deep Within Progressing Plaques

Intravital imaging presented a limited time interval for the examination of monocyte and macrophage motility within the plaque. Therefore, approaches allowing for longer tracking needed to be implemented. We had previously established that macrophage loss from plaques can be triggered by virally induced apoE expression in plaque-bearing ApoE$^{-/-}$ mice. Adeno-associated viral 8-ApoE viral transduction was efficient at reversing plasma cholesterol levels rapidly and stably[15] in male mice (Figure IIA and IIB in the online-only Data Supplement), with the labeling and infection protocol outlined in Figure IIC in the online-only Data Supplement. Particles carried by macrophages are not removed from plaques during the period of macrophage loss in this model,[13] leading us to conclude that migratory egress of macrophages was not necessary for their removal and such migration was not occurring in this model. However, on subsequent closer inspection of plaque sections in these experiments there was a striking pattern in which particles appeared further from the lumen during disease progression (empty adenoviral vector; Figure 2Aa) and near the lumen in the regression treatment (ad-hApoE3; Figure 2Bb). Importantly, beads were observed to be largely present in the cytoplasm of macrophages within the plaque for either treatment condition (Figure 2C). Indeed, quantification of particle distance from the lumen confirmed the deeper positioning of particles in the empty adenoviral vector group compared with the ad-hApoE3 group (Figure 2D). We further confirmed that total bead counts in the various groups were not statistically different, as expected[13] (Figure 2E).

We initially wondered whether macrophages containing beads as cargo had wandered closer to the lumen during regression even if they had not egressed with such cargo. However, we negated this possibility when we quantified whether the particles were deeper within the plaques when their position was determined relative to the internal elastic laminal border just above the internal elastic lamina and

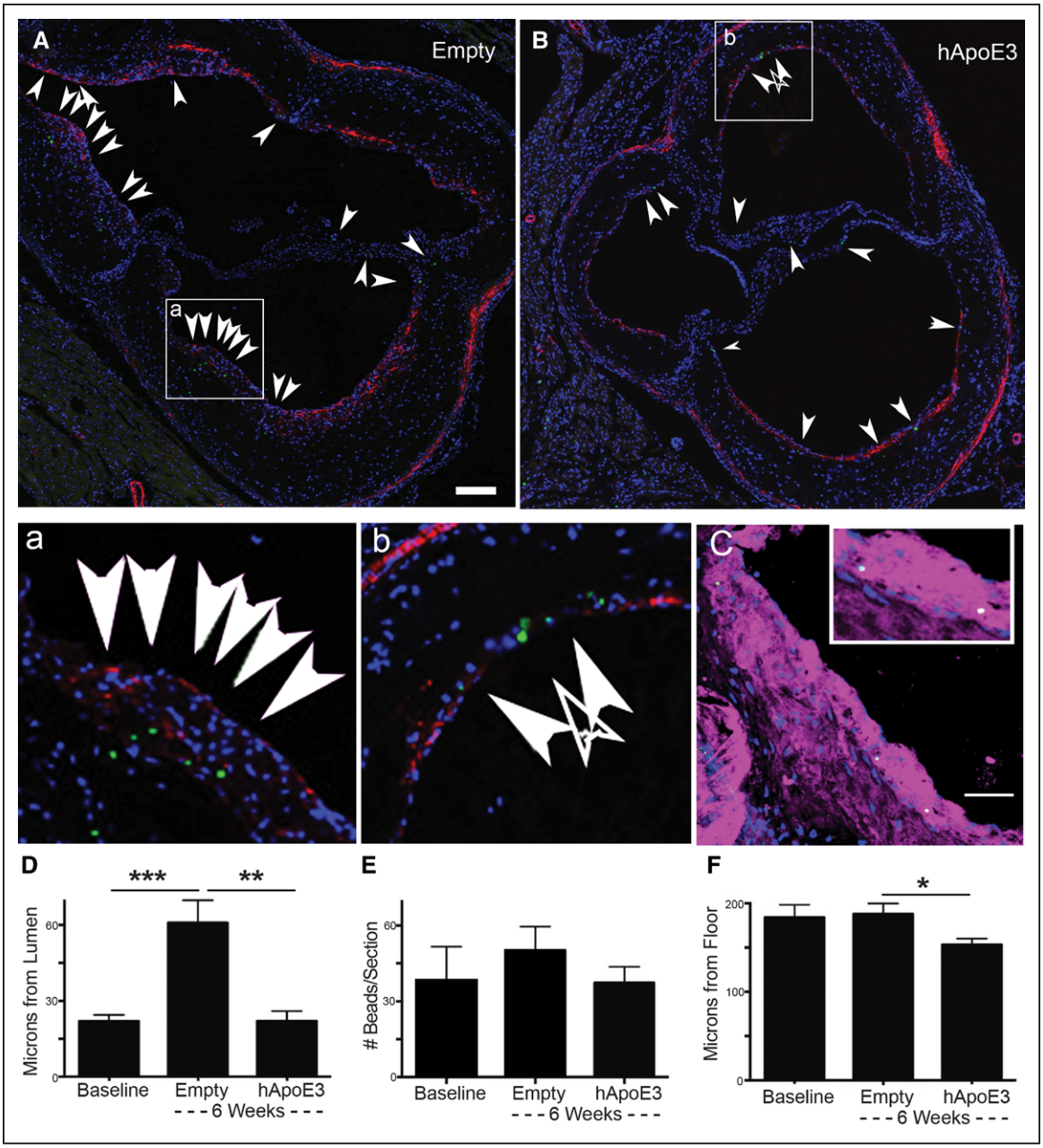

Figure 2. Positional tracking using phagocytic cargo labeling suggests little displacement of central plaque macrophages over several weeks during plaque progression or regression. **A** and **B**, Image shows aortic sinus plaque section from ApoE$^{-/-}$ mice treated with adenovirus, after model II in Figure IIC in the online-only Data Supplement, that was empty (control, **A**) or that encoded hApoE3 to promote regression (**B**). Tissues were recovered 6 wk after monocyte labeling with green beads and vector treatment. Arrows point to green beads within plaques (marked by green dots), including beads within the valve leaflets, although beads in leaflets were not counted as being part of the plaque. To help highlight the floor of the plaque, counterstaining for smooth muscle actin was included (red). Nuclei are stained with DAPI (4',6-diamidino-2-phenylindole; blue). Insets (2**a** and 2**b**) show higher magnification of images to visualize green bead deposition in the plaque. Scale bar, 50 μm. **C**, Green beads within plaques were present within macrophage-rich regions, identified by CD115 and MOMA2 (macrophages/monocytes monoclonal antibody) costaining (magenta). Sample from an empty-vector treated animal. Nuclei stained by DAPI in blue, scale bar 10 μm. **D**, Bead distance from the plaque lumen was assessed 5 d after bead labeling of blood monocytes, just before adenovirus treatment (baseline) or 6 wk after empty or ApoE3 vectors were administered. **E**, Total beads in plaque sections were enumerated. **F**, Distance of beads from the floor of the plaque, defined by elastic lamina and muscle layer, was quantified. Data are from a single experiment in which 7 to 10 mice were included in each group. Experiments are representative of a total of 6 independent experiments performed, each with slightly different timing or design, but all providing support for the conclusions drawn here. Statistics were performed by 2-way ANOVA with Tukey correction for multiple comparison test (*P* value, *≤0.0332, **≤0.0021, and ***≤0.0002).

smooth muscle actin staining medial layer (Figure 2A, 2B, and 2F). In this assessment, beads in the regressing group were slightly closer to the plaque floor, perhaps because of the modest reduction in plaque area during regression (Figure 2F). Most significantly, the distance of the cargo from the floor of the plaque was the same at day 5 after labeling (baseline) and did not change for the following 6 weeks of HFD feeding in the empty vector-treated animals

(Figure 2F). Thus, the apparent penetration of bead-bearing phagocytes to progressing plaques and the apparent retention (or return) of phagocytic cargo to the vessel lumen in regressive conditions was an optical aberration related to luminal growth of the plaque, without bead-bearing cells moving deeper into plaque. The difference in bead positioning relative to the endothelial lumen during plaque regression versus progression, then, could be explained by the cessation of monocyte recruitment that is induced by ad-hApoE3.[13] That is, overall, the data suggested that particles brought in by monocyte-derived macrophages have no net displacement in the depth of the plaque (we have no landmarks to assess lateral movement) within plaques for weeks. Instead, under conditions when monocyte recruitment is robust, the particle-bearing cells are layered on by the newly recruited cells. However, if monocyte recruitment abates, such as in our regression model, the phagocytic cargo remains relatively nearer the vessel lumen.

To further test the concept that macrophage positioning in plaques is primarily the product of a layering phenomenon that does not allow for significant penetration of newly recruited cells into the deeper layers of the plaque, we performed experiments with ApoE$^{-/-}$ mice on HFD for different periods in which particle labeling of monocytes occurred in 2 kinetic waves using green or red particles in succession (modeled in Figure III in the online-only Data Supplement). Just as above, this approach allows for measurements in the z axis to quantify depth within the plaques, but does not allow for measurements of side-to-side motility. Labeling of monocytes early in plaque progression (green beads) resulted in labeled cells positioned nearer the plaque floor than the luminal border (Figure 3A). Conversely, later labeling (red beads) showed positioning of the second wave of particles nearer the endothelial surface (Figure 3B and 3C). In addition to the bead labeling of monocytes at different time periods resulting in bead positioning within plaque being restricted by relative location, we observed no scenario in which a cell had taken up both bead colors, arguing against significant bead transfer, or cell death and bead efferocytosis by a phagocyte containing a bead of another color in the time points studied. Furthermore, the dramatic separation in localization of the red and green beads supports limited access of circulating monocytes to established regions of the plaque. Taken together, these data support that macrophage motility in the plaque z axis is low. If it occurs, macrophage motility leads to no net displacement in macrophage positioning within plaques.

Phagocytic Cargo Shows Minimal Gene Expression Changes on Circulating Monocytes

Finally, we performed quality control experiments to assess whether the phagocytic labeling of macrophages with bead particles might strongly alter their phenotype. Previous studies using plain polystyrene particle-labeled monocytes to assess recruitment into tissues have demonstrated that bead labeling did not affect the ability of monocytes to enter tissues,[21] and particle uptake did not activate p38/MAPK (mitogen-activated protein kinase) or NFκB (nuclear factor kappa B) pathways.[22] Placement of particles in the airway does not induce inflammation, as indicated by lack of neutrophil recruitment.[23] However, the possibility remains that bead labeling could have effects on global gene expression profiles. To address this prospect, we performed gene expression profiling of classical and nonclassical monocytes that had taken up latex particle in vivo against cells from the same mouse that had not taken up particles. Unbiased clustering analysis of gene expression data revealed the primary driver of population differences (principal component 1) was the cell type being assessed (classical versus nonclassical) and the presence of latex beads was a secondary function (principal component 2) of diversity in the array (Figure 4A). In classical monocytes, only 5 individual mRNA transcripts were significantly upregulated by bead uptake, including Spic, Fabp5, and 3 complement component transcripts C1qa, C1qb, C1qc. There were no significant transcripts downregulated. With respect to nonclassical monocytes, bead labeling-induced significant

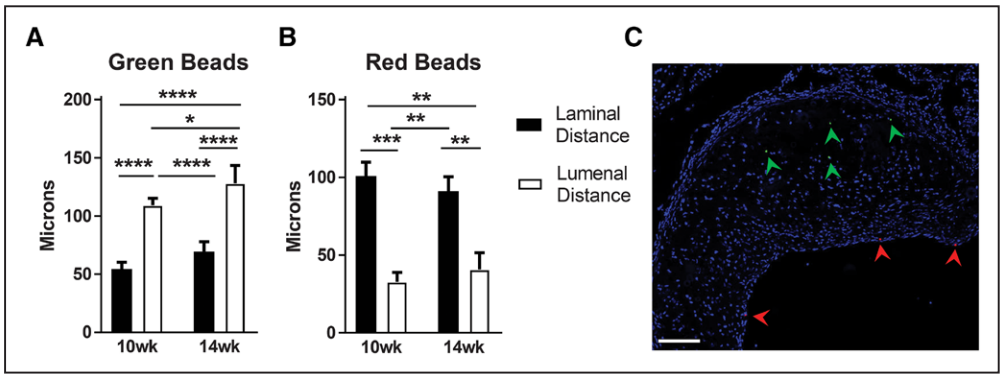

Figure 3. Positional tracking of phagocytic cargo shows minimal displacement in progressing plaques in relation to the plaque laminal boarder. **A** and **B**) Green beads were used to label blood monocytes given 2 wk after ApoE$^{-/-}$ mice were transitioned to a high-fat diet (HFD) after weaning. Then, in the same mice, red beads were used to label monocytes 7 d before the end of the 10- or 14-wk period of HFD feeding (modeled in Figure III in the online-only Data Supplement). The position of each bead type was recorded with respect to plaque lumen or plaque floor, with representative image (**C**) showing localization of green and red beads in plaque (marked by arrows, scale bar 100 μm). Displayed data combine 2 independent experiments using 2 time points (10 or 14 wk of HFD), with experimental group sizes of 4 to 6 mice. For each mouse, 5 sections were charted with ≈20 to 40 beads of each color per section and distance measurements averaged for each mouse. Statistics were performed by 2-way ANOVA with Tukey correction for multiple comparison test (*P* value, *≤0.0332, **≤0.0021, ***≤0.0002, and ****≤0.00 001).

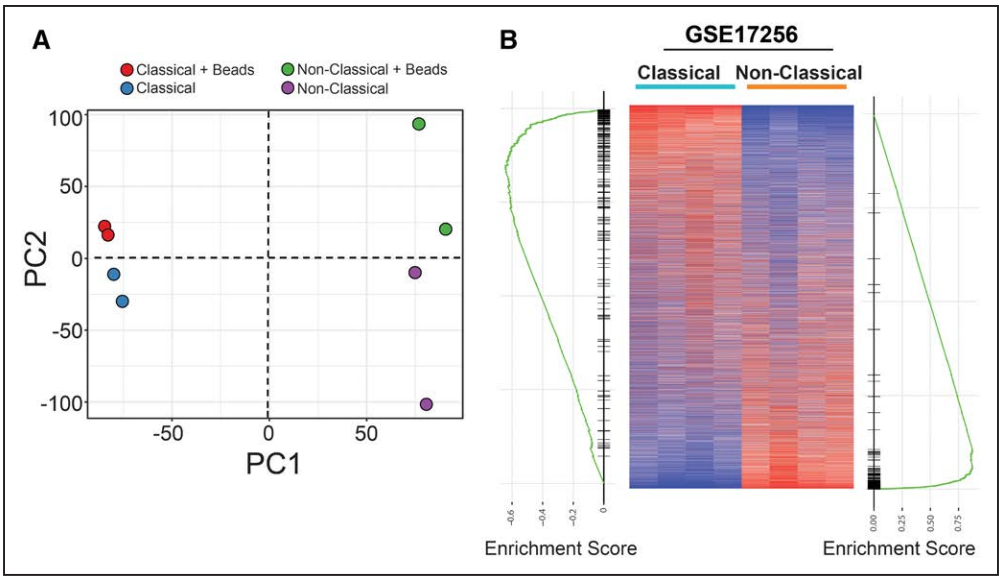

Figure 4. Monocytes show minimal gene expression changes in response to bead loading in vivo. Classical and nonclassical monocytes, which were loaded with beads or not (cntl) were assayed for gene expression changes associated with the presence of beads. **A**, Principle component analysis analysis shows unbiased clustering of samples. **B**, Monocyte gene expression data from wild-type untreated mice (heatmap, GSE17256) was compared with the top 150 genes associated with classical or nonclassical monocytes from animals that were treated with bead labeling approach. Comparison showed significant enrichment of genes between sample groups, with the **left** gene set enrichment analysis (GSEA) plot representing classical monocyte genes and **right** GSEA plot representing nonclassical monocyte genes.

upregulation of CD209a, Klrd1, Slc40a1, F13a1, and Vcan. Again, there were no significantly downregulated transcripts in bead-labeled nonclassical monocytes compared with their unlabeled counterparts. With these few changes in gene expression, pathway analysis yielded no pathways that were significantly altered using an adjusted P value <0.01.

Given that the data collected on the impact of bead labeling was performed on monocytes with or without bead uptake in mice that had been treated so as to label monocytes, we performed further analysis to determine whether there were gene expression changes in association with monocytes whose gene expression was analyzed from previously unmanipulated mice.[24] Using the top 150 genes enriched in classical or nonclassical monocytes from mice subjected to bead labeling, we assessed the distribution of these genes against previously published data set of monocytes from untreated mice (Figure 4B). Heat maps of rank-listed genes in either classical or nonclassical monocytes revealed a high degree of enrichment between experimental groups comparing monocytes from unmanipulated and bead-manipulated mice. Altogether, these data suggest that neither the labeling of monocytes with latex beads nor the procedure associated with it leads to dramatic changes in overall gene expression compared with circulating monocytes from naïve mice. Thus, the conclusions drawn regarding the relative immobility of monocyte-derived cells in plaques is not likely an artifact of changes associated with bead labeling.

Discussion

Using an established model of plaque regression, this study brings technical and conceptual advances to our understanding of experimental atherosclerosis. The underlying question and dilemma driving the study was to better understand the migratory capacity and behavior of macrophages in plaques. Intravital imaging of atherosclerotic plaques is challenging, not least because of the need to confront motion associated with breathing and heart rhythm in the arterial tree. However, using different approaches, these hurdles are being overcome in different groups, largely either with the use of software that collects images in rhythm with the heart beat[7] or with physical stabilization of arterial tissue to reduce motion.[6,11] We developed a preparation capable of direct imaging of established plaque in the carotid artery. To our knowledge, our preparation is the first to image HFD-induced established plaques native to the animal being evaluated, as compared with injury-induced plaques,[6] transplanted vessels,[11] or monocyte interactions with the vessel wall before plaque progression.[8] Having developed a stable and high-resolution imaging approach, we found that macrophages piled in clusters within the plaque were highly sessile, displaying minimal net displacement. Smaller, monocyte-like cells were motile in regions adjacent to the established plaque. At least a few of these cells may have been undergoing recruitment and integration into plaques. However, even these monocytes, while motile, did not seem to penetrate deep into the plaque.

These results motivated us to test the migratory potential of plaque macrophages using long-term progressive or regressive conditions. We charted the position of phagocytic bead cargo transported into plaque by recruited monocytes and asked whether there were z-axis shifts (shifts in depth) in cargo localization within the plaque after progressive or regressive conditions. If random motility occurred in plaque macrophages throughout the plaque (including plaque depth),[25] or if directed migration promoted movement to a particular part of plaque, we would expect to be able to quantify

this motility as a net displacement of phagocytic cargo over time. With the data showing no depth displacement in bead localization within the plaque over up to a 6-week period, we conclude that macrophage motility in plaques is limited. Previous studies have noted that macrophage phenotype is segregated between regions within plaque, with classically activated macrophage found near the necrotic core/unstable plaque regions and alternatively activated macrophages near the border/stable regions.[26] Our data suggest that these observations may be explained by stable, positional differences in phenotype: the microenvironment of the plaque controls the macrophage phenotype and this phenotype is not diluted by the ability of macrophages to readily relocate to other areas that would simultaneously allow macrophages with different phenotypes to mix. That macrophages may take on particular functional phenotypes as a result of their positioning within plaques underscores the concept that although we conclude that macrophages are largely immobile, they are not functionally inert, but indeed may carry out pivotal roles in the spatial confines in which they reside.

It remains unclear whether the motile monocytes observed near the surface of the plaque shoulders frequently or infrequently integrate into the plaque itself. However, some smaller cells were observed having lost mobility at the edges of the plaque, suggesting they may have begun differentiation programs to develop into foamy macrophages within the arterial wall. Clear evidence of monocyte recruitment into and integration within plaques was not observed in the videos we obtained. This is an important issue as a picture starts to emerge about the dynamics of changes that occur within plaques. In particular, the data presented here, when considered with the literature at large, most strongly support a model in which monocyte differentiation to macrophages results in cells with a limited range of mobility regardless of whether a plaque is regressing, creating not a swarm as seen in lymph nodes for lymphocytes,[25] but rather a zone of collected cells with fixed spatial arrangements, much as reported in liver granulomas.[5] The data presented here fit with our previous observation that congenically marked monocytes layer over older macrophages in plaques.[27] Furthermore, it is unlikely that presence of the bead within phagocytes causes sessility because we have reported numerous instances in which beads were carried by mononuclear phagocytes for long distances.[21,28–30] Additionally, we performed gene expression profile analysis between monocytes loaded with beads and those that had not and found minimal changes in overall gene expression, which was consistent with previous reports suggesting that bead loading had not dramatic effects on activation or survival pathways.[21,22] Because our bead tracking studies included analysis of regressing conditions and these data support relative immobility of macrophages during disease reversal, it is unlikely that plaque regression is associated with a marked increase in migratory capacity for most plaque macrophages.

With respect to the use of beads to track the position of macrophages in plaques, 1 immediately may consider whether the technique is limited by the possibility that beads are transferred from 1 macrophage to another under conditions in which the bead-carrying macrophage may undergo death. However, engulfment of beads or engulfment of a bead-bearing dying macrophage would necessarily require that the efferocytic macrophage localize close to a dying macrophage. Once engulfed, the efferocytic macrophage would in turn have the potential to migrate or remain relatively immobile. When this consideration is taken into account, it seems unlikely that even death of the original macrophage would greatly alter the interpretation of the experiment, as long as the beads remained within macrophages as a population, which we show is the case. To guard against the possibility that the phagocytic labeling technique might yield incorrect conclusions, we developed a live imaging approach. The live imaging supported the conclusion that macrophages in plaques are scarcely mobile.

The issue of relative mobility is important because once macrophages have differentiated and thereby become spatially confined, they may become vulnerable to adverse changes within their microenvironment that they cannot escape, including changes in which incoming macrophages pile over them. Indeed, the inability to escape may be a force underlying the development of a necrotic core and its reticence for clearance. Indeed, the 2 instances where macrophage motility has been defined as limited, granulomas[5] and the present work on atherosclerotic plaque, are 2 instances that are prone to emergence of necrotic core. Future incorporation of our findings into mathematical modeling of plaque progression may allow us to better understand conditions that control plaque vulnerability to rupture.

Acknowledgments

We thank D.J. Rader (University of Pennsylvania) for kindly providing ApoE-encoding adenoviral vector. We also thank Anton Kyrychenko for designing and drawing the graphical abstract.

Sources of Funding

Major support for this work was supplied by National Institutes of Health (NIH) R01/R37 AI049653 and NIH RO1 HL118206 to G.J. Randolph. Additional support to G.J. Randolph includes NIH DP1DK109668. J.W. Williams was supported by NIH training grant 2T32DK007120-41, American Heart Association (AHA) grant 17POST33410473, and NIH K99HL138163. A. Elvington was supported by NIH training grant T32-HL07081-38 and B.H. Zinselmeyer was supported by AHA grant 16SDGG30480008.

Disclosures

None.

References

1. Randolph GJ. Mechanisms that regulate macrophage burden in atherosclerosis. *Circ Res*. 2014;114:1757–1771. doi: 10.1161/CIRCRESAHA.114.301174.
2. Hilgendorf I, Swirski FK, Robbins CS. Monocyte fate in atherosclerosis. *Arterioscler Thromb Vasc Biol*. 2015;35:272–279. doi: 10.1161/ATVBAHA.114.303565.
3. Ai D, Jiang H, Westerterp M, Murphy AJ, Wang M, Ganda A, Abramowicz S, Welch C, Almazan F, Zhu Y, Miller YI, Tall AR. Disruption of mammalian target of rapamycin complex 1 in macrophages decreases chemokine gene expression and atherosclerosis. *Circ Res*. 2014;114:1576–1584. doi: 10.1161/CIRCRESAHA.114.302313.
4. Virmani R, Burke AP, Farb A, Kolodgie FD. Pathology of the vulnerable plaque. *J Am Coll Cardiol*. 2006;47(8 suppl):C13–C18. doi: 10.1016/j.jacc.2005.10.065.
5. Egen JG, Rothfuchs AG, Feng CG, Winter N, Sher A, Germain RN. Macrophage and T cell dynamics during the development and

disintegration of mycobacterial granulomas. *Immunity*. 2008;28:271–284. doi: 10.1016/j.immuni.2007.12.010.
6. Chèvre R, González-Granado JM, Megens RT, Sreeramkumar V, Silvestre-Roig C, Molina-Sánchez P, Weber C, Soehnlein O, Hidalgo A, Andrés V. High-resolution imaging of intravascular atherogenic inflammation in live mice. *Circ Res*. 2014;114:770–779. doi: 10.1161/CIRCRESAHA.114.302590.
7. McArdle S, Chodaczek G, Ray N, Ley K. Intravital live cell triggered imaging system reveals monocyte patrolling and macrophage migration in atherosclerotic arteries. *J Biomed Opt*. 2015;20:26005. doi: 10.1117/1.JBO.20.2.026005.
8. Quintar A, McArdle S, Wolf D, Marki A, Ehinger E, Vassallo M, Miller J, Mikulski Z, Ley K, Buscher K. Endothelial protective monocyte patrolling in large arteries intensified by Western diet and atherosclerosis. *Circ Res*. 2017;120:1789–1799. doi: 10.1161/CIRCRESAHA.117.310739.
9. Marcovecchio PM, Thomas GD, Mikulski Z, Ehinger E, Mueller KAL, Blatchley A, Wu R, Miller YI, Nguyen AT, Taylor AM, McNamara CA, Ley K, Hedrick CC. Scavenger receptor CD36 directs nonclassical monocyte patrolling along the endothelium during early atherogenesis. *Arterioscler Thromb Vasc Biol*. 2017;37:2043–2052. doi: 10.1161/ATVBAHA.117.309123.
10. Williams JW, Randolph GJ, Zinselmeyer BH. A polecat's view of patrolling monocytes. *Circ Res*. 2017;120:1699–1701. doi: 10.1161/CIRCRESAHA.117.311021.
11. Li W, Luehmann HP, Hsiao HM, Tanaka S, Higashikubo R, Gauthier JM, Sultan D, Lavine KJ, Brody SL, Gelman AE, Gropler RJ, Liu Y, Kreisel D. Visualization of monocytic cells in regressing atherosclerotic plaques by intravital 2-photon and positron emission tomography-based imaging-brief report. *Arterioscler Thromb Vasc Biol*. 2018;38:1030–1036. doi: 10.1161/ATVBAHA.117.310517.
12. Satpathy AT, Briseño CG, Lee JS, et al. Notch2-dependent classical dendritic cells orchestrate intestinal immunity to attaching-and-effacing bacterial pathogens. *Nat Immunol*. 2013;14:937–948. doi: 10.1038/ni.2679.
13. Potteaux S, Gautier EL, Hutchison SB, van Rooijen N, Rader DJ, Thomas MJ, Sorci-Thomas MG, Randolph GJ. Suppressed monocyte recruitment drives macrophage removal from atherosclerotic plaques of Apoe-/- mice during disease regression. *J Clin Invest*. 2011;121:2025–2036. doi: 10.1172/JCI43802.
14. Tsukamoto K, Smith P, Glick JM, Rader DJ. Liver-directed gene transfer and prolonged expression of three major human ApoE isoforms in ApoE-deficient mice. *J Clin Invest*. 1997;100:107–114. doi: 10.1172/JCI119501.
15. Kim IH, Józkowicz A, Piedra PA, Oka K, Chan L. Lifetime correction of genetic deficiency in mice with a single injection of helper-dependent adenoviral vector. *Proc Natl Acad Sci USA*. 2001;98:13282–13287. doi: 10.1073/pnas.241506298.
16. Gräbner R, Lötzer K, Döpping S, et al. Lymphotoxin beta receptor signaling promotes tertiary lymphoid organogenesis in the aorta adventitia of aged ApoE-/- mice. *J Exp Med*. 2009;206:233–248. doi: 10.1084/jem.20080752.
17. Berman ME, Muller WA. Ligation of platelet/endothelial cell adhesion molecule 1 (PECAM-1/CD31) on monocytes and neutrophils increases binding capacity of leukocyte CR3 (CD11b/CD18). *J Immunol*. 1995;154:299–307.
18. Haka AS, Potteaux S, Fraser H, Randolph GJ, Maxfield FR. Quantitative analysis of monocyte subpopulations in murine atherosclerotic plaques by multiphoton microscopy. *PLoS One*. 2012;7:e44823. doi: 10.1371/journal.pone.0044823.
19. Huang CK, Pang H, Wang L, Niu Y, Luo J, Chang E, Sparks JD, Lee SO, Chang C. New therapy via targeting androgen receptor in monocytes/macrophages to battle atherosclerosis. *Hypertension*. 2014;63:1345–1353. doi: 10.1161/HYPERTENSIONAHA.113.02804.
20. Jonasson L, Holm J, Skalli O, Bondjers G, Hansson GK. Regional accumulations of T cells, macrophages, and smooth muscle cells in the human atherosclerotic plaque. *Arteriosclerosis*. 1986;6:131–138.
21. Tacke F, Alvarez D, Kaplan TJ, Jakubzick C, Spanbroek R, Llodra J, Garin A, Liu J, Mack M, van Rooijen N, Lira SA, Habenicht AJ, Randolph GJ. Monocyte subsets differentially employ CCR2, CCR5, and CX3CR1 to accumulate within atherosclerotic plaques. *J Clin Invest*. 2007;117:185–194. doi: 10.1172/JCI28549.
22. Yates RM, Russell DG. Phagosome maturation proceeds independently of stimulation of toll-like receptors 2 and 4. *Immunity*. 2005;23:409–417. doi: 10.1016/j.immuni.2005.09.007.
23. Jakubzick C, Helft J, Kaplan TJ, Randolph GJ. Optimization of methods to study pulmonary dendritic cell migration reveals distinct capacities of DC subsets to acquire soluble versus particulate antigen. *J Immunol Methods*. 2008;337:121–131. doi: 10.1016/j.jim.2008.07.005.
24. Ingersoll MA, Spanbroek R, Lottaz C, Gautier EL, Frankenberger M, Hoffmann R, Lang R, Haniffa M, Collin M, Tacke F, Habenicht AJ, Ziegler-Heitbrock L, Randolph GJ. Comparison of gene expression profiles between human and mouse monocyte subsets. *Blood*. 2010;115:e10–e19. doi: 10.1182/blood-2009-07-235028.
25. Cahalan MD, Parker I, Wei SH, Miller MJ. Real-time imaging of lymphocytes in vivo. *Curr Opin Immunol*. 2003;15:372–377.
26. Chinetti-Gbaguidi G, Colin S, Staels B. Macrophage subsets in atherosclerosis. *Nat Rev Cardiol*. 2015;12:10–17. doi: 10.1038/nrcardio.2014.173.
27. Llodrá J, Angeli V, Liu J, Trogan E, Fisher EA, Randolph GJ. Emigration of monocyte-derived cells from atherosclerotic lesions characterizes regressive, but not progressive, plaques. *Proc Natl Acad Sci USA*. 2004;101:11779–11784. doi: 10.1073/pnas.0403259101.
28. Jakubzick C, Gautier EL, Gibbings SL, et al. Minimal differentiation of classical monocytes as they survey steady-state tissues and transport antigen to lymph nodes. *Immunity*. 2013;39:599–610. doi: 10.1016/j.immuni.2013.08.007.
29. Jakubzick C, Tacke F, Llodra J, van Rooijen N, Randolph GJ. Modulation of dendritic cell trafficking to and from the airways. *J Immunol*. 2006;176:3578–3584.
30. Randolph GJ, Inaba K, Robbiani DF, Steinman RM, Muller WA. Differentiation of phagocytic monocytes into lymph node dendritic cells in vivo. *Immunity*. 1999;11:753–761.

Highlights

- Intravital imaging of carotid atherosclerotic plaques displays motile monocytes and sessile foamy macrophages.
- Monocytes, tracked with a long-term label, are recruited to the superficial surface of atherosclerotic plaques and as a population have limited penetration into the plaque, resulting in a tree ring-like growth pattern for atherosclerotic plaque as incoming monocytes overlay earlier recruited ones.
- The spatial confinement of recruited monocytes is operative in both regressing and progressing plaques, indicating that limited motility is not linked to hypercholesterolemia or plaque status.
- Limited spatial dynamics may impact macrophage survival and phagocytic cleanup of other macrophages, and thus necrotic core formation because macrophages have limited capacity to remove themselves from environments that may impinge on viability.